Life Sciences 232 (2019) 116664

Contents lists available at ScienceDirect

Life Sciences

journal homepage: www.elsevier.com/locate/lifescie

# MicroRNA-99a-5p alleviates atherosclerosis *via* regulating Homeobox A1

Zhiyang Han[a], Yinghui Guan[a], Bing Liu[a], Yu Lin[a], Yan Yan[a], Haijun Wang[a], Hengzhen Wang[a], Bao Jing[b,*]

[a] Department of General Surgery, The First Affiliated Hospital of Harbin Medical University, Harbin 150001, People's Republic of China
[b] Department of Vascular Surgery, The First Affiliated Hospital of Harbin Medical University, Harbin 150070, People's Republic of China

ARTICLE INFO

*Keywords:*
MicroRNA-99a-5p
Homeobox A1
Atherosclerosis
Human aortic smooth muscle cells
Apolipoprotein E knockout mice

ABSTRACT

*Aims:* MicroRNAs have been demonstrated to be involved in the development of atherosclerosis. The present study aimed to evaluate the effect of miR-99a-5p and its target gene Homeobox A1 (HOXA1) in atherosclerosis.
*Main methods:* The biological functions of miR-99a-5p on human aortic smooth muscle cells (ASMCs) were assessed by MTT, wound healing and transwell assays. The target genes of microRNAs were predicted by TargetScan and miRDB. The binding of miR-99a-5p and HOXA1 was confirmed by luciferase reporter assay. In the *in vivo* study, high-fat diet-induced atherosclerosis model was established in Apolipoprotein E knockout mice. Hematoxylin-eosin (H&E), oil Red O and Masson trichrome staining were performed for determination of atherosclerotic lesion. The levels of miR-99a-5p and HOXA1 mRNA were detected by real-time PCR. HOXA1 and migration-associated protein levels were detected by western blot or immunohistochemistry analysis.
*Key findings:* MiR-99a-5p inhibited HOXA1 expression by targeting 3′UTR of HOXA1 mRNA. Enforced HOXA1 significantly promoted the proliferation, migration, and invasion of ASMCs. Furthermore, miR-99a-5p overexpression inhibited the proliferation, migration, and invasion of ASMCs stimulated by HOXA1, whereas miR-99a-5p inhibition reversed the effects of HOXA1 knockdown on these behaviours of ASMCs. *In vivo*, the specific overexpression of miR-99a-5p significantly abated atherosclerotic lesions formatted, accompanied with a significant down-regulation of HOXA1 mRNA and protein expression levels.
*Significance:* We demonstrate for first time that miR-99a-5p may serve as a potential inhibitor of the atherosclerosis, and miR-99a-5p plays its role partially through targeting HOXA1.

## 1. Introduction

Atherosclerosis is an age-related artery disease which is characterized by the thickening, hardening, stenosis and the formation of atherosclerotic plaques of the arteries [1,2]. It is the leading cause of cardiovascular, cerebrovascular and peripheral arterial diseases. Although various therapeutic techniques for the treatment of atherosclerosis have been developed, the risk of diseases induced by atherosclerosis and its complications remain at a high level. Therefore, it is necessary to further explore the underlying complex molecular mechanism and find novel therapeutic targets.

MicroRNAs (miRNAs) are a class of non-coding small RNAs of 19–25 nucleotides in length that modulate cell apoptosis, proliferation and differentiation by completely or incompletely pairing with the 3′ untranslation region (3′ UTR) of the target gene mRNA [3,4]. Increasing evidences have indicated that miRNAs participate in the development of atherosclerosis. For instance, miR-let-7g attenuates atherosclerosis partially by targeting the LOX-1 signalling pathway [5]. While miR-24 accelerates atherosclerosis by inhibiting lipid uptake [6]. MiR-99a-5p is a tumour suppressor and has been widely studied in various kinds of cancers [7–9]. In a recent study, miR-99a-5p has been reported to inhibit insulin-induced proliferation, migration and dedifferentiation in vascular smooth muscle cells (VSMCs) [10]. Phenotypic changes of VSMCs have been suggested to play key roles in the pathogenesis and progression of atherosclerosis [11,12], and inhibition of the phenotypic switch of VSMCs is considered as a therapeutic target for atherosclerosis treatment [13,14]. Thus, we hypothesize that miR-99a-5p may participate in the process of atherosclerosis.

HOX proteins are a series of transcription factors required for the patterning of the body plan in the embryo [15,16], and are involved in vascular wall-resident multipotent stem cell differentiation into smooth muscle cells [17]. HOXA1, one of the HOX family members, plays critical roles during early vertebrate development. It is involved in various biological processes, such as cancer cells growth, migration and

* Corresponding author at: Department of Vascular Surgery, The First Affiliated Hospital of Harbin Medical University, 2075 Qunli Seventh Avenue, Harbin 150070, People's Republic of China.
*E-mail address:* jingbao06@126.com (B. Jing).

https://doi.org/10.1016/j.lfs.2019.116664
Received 22 March 2019; Received in revised form 10 July 2019; Accepted 15 July 2019
Available online 17 July 2019

**Table 1**
Primers for real-time PCR.

| Gene name | | Primer sequence |
|---|---|---|
| Has-miR-99a-5p | Forward primer (5′-3′) | GTGACAACCCGTAGATCCGATC |
| | Reverse primer (5′-3′) | GTGCAGGGTCCGAGGTATTC |
| Mmu-miR-99a-5p | Forward primer (5′-3′) | GTGACAACCCGTAGATCCGATC |
| | Reverse primer (5′-3′) | GTGCAGGGTCCGAGGTATTC |
| Homo HOXA1 | Forward primer (5′-3′) | CAACGAGACCCAAGTGAAGATC |
| | Reverse primer (5′-3′) | AAGGAACGCAGGGCGAAGA |
| Mus HOXA1 | Forward primer (5′-3′) | CACCACCACCATCACCACC |
| | Reverse primer (5′-3′) | CCAGAGTAAACAGCGGGAGC |

Note: miR-99a-5p: microRNA-99a-5p; HOXA1: Homeobox A1.

invasion [18,19]. Recently, HOXA1 has been found to be up-regulated in the athero-susceptible regions of the inner aortic arch and aorto-renal branches [20], which indicates that HOXA1 may be involved in the pathological mechanisms of atherosclerosis. Additionally, previous studies have indicated that HOXA1 is a target of miR-99a-5p in epithelial cells and in breast cancer cells [21,22]. However, the role of miR-99a-5p/HOXA1 in atherosclerosis has not been elucidated. In the present study, we investigated the effects of miR-99a-5p/HOXA1 on the phenotype of VSMCs *in vitro* and whether overexpression of miR-99a-5p could attenuate atherosclerosis *in vivo*.

## 2. Materials and methods

### 2.1. Cell culture of human aortic smooth muscle cells (ASMCs)

Primary human ASMCs purchased from Shanghai Zhong Qiao Xin Zhou Biotechnology Co., Ltd. (Shanghai, China) were cultured in F12K complete medium (Sciencell, San Diego, CA, USA) at 37 °C in a humidified 5% $CO_2$ incubator. Immunofluorescence assay was performed for the detection of smooth muscle α-actin (SM α-actin) and smooth muscle 22 alpha (SM-22α) expression to identify the contractile phenotype of ASMCs (Supplemental Fig. 1).

### 2.2. Bioinformatics

The TargetScan (http://www.targetscan.org) and miRDB (http://www.mirdb.org) software programs were applied to predict the miR-99a-5p putative target genes.

### 2.3. Cell transfection

Cells were trypsinized, counted and seeded into six-well plates the day before transfection to ensure cell confluence reached 70%.

For overexpression of HOXA1, the human HOXA1 coding sequence was inserted into the pcDNA3.1 (+) vector (pcDNA3.1-HOXA1, Clontech, Palo Alto, CA, USA). HOXA1 siRNA (small interfering RNA, si-HOXA1) was used to knock down HOXA1. For overexpression or knockdown of miR-99a-5p (Accession Number: MIMAT0000097), the miR-99a-5p agomir, miR-99a-5p antagomir, and their negative control (NC) agomir were purchased from GenePharma Co., Ltd. (Shanghai, China). The transfection and co-transfection were performed using Lipofectamine RNAiMAX or Lipofectamine 3000 (Invitrogen, Carlsbad, CA, USA).

### 2.4. Cell proliferation assay

3-(4,5-Dimethylthiazol-2-yl)-2,5-diphenyltetrazolium bromide (MTT) assay was conducted to detect cell proliferation. ASMCs were seeded into 96-well plates at a density of $3 \times 10^3$ cells/well. At 24 h after transfection, the cultures were continued for 24, 48, and 72 h. At each specific time point, the cell medium was replaced with DMEM complete medium containing MTT (0.5 mg/ml, Sigma, St. Louis, MO,

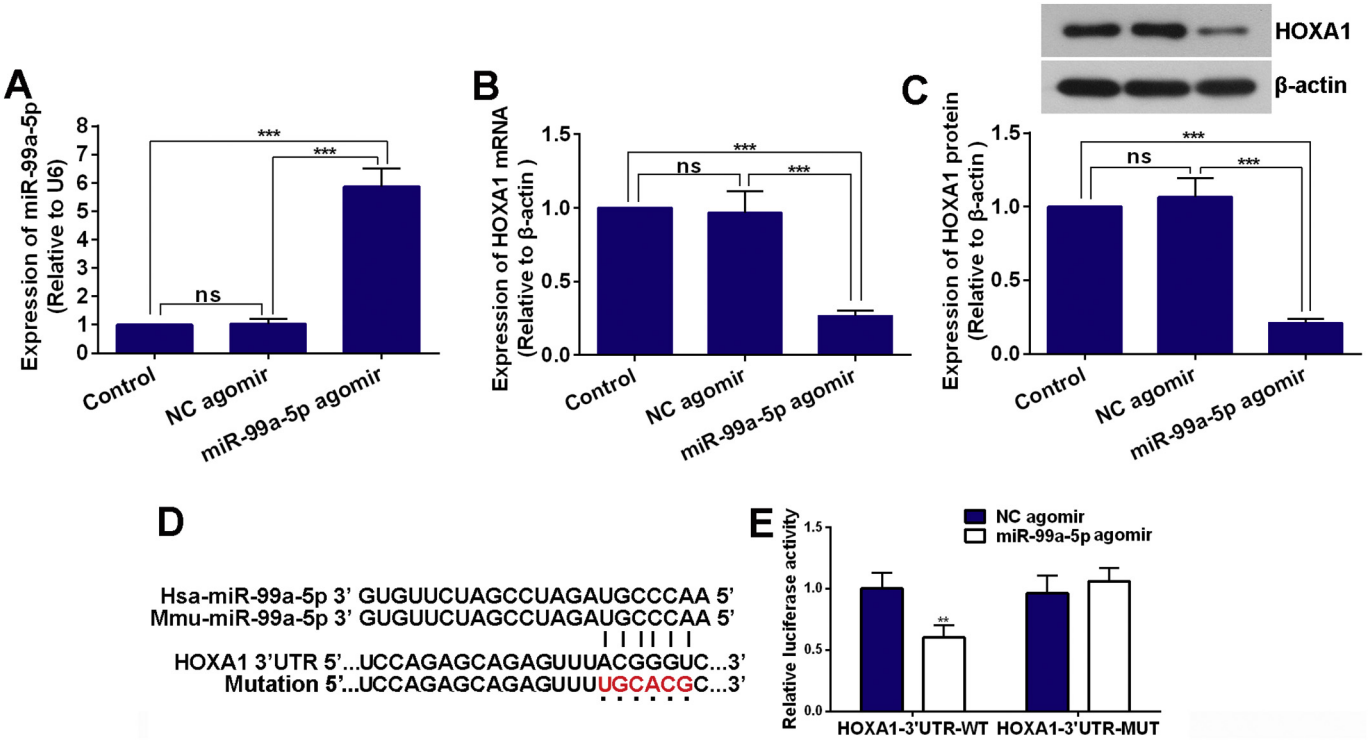


**Fig. 1.** HOXA1 is a direct target of miR-99a-5p. (A) Relative miR-99a-5p level in ASMCs transfected with NC agomir or miR-99a-5p agomir was assessed by real-time PCR. (B and C) Relative mRNA and protein levels of HOXA1 were assessed by real-time PCR and western blot in ASMCs transfected with NC agomir or miR-99a-5p agomir. (D) 3′ UTR of HOXA1 was predicted to contain a complementary region of miR-99a-5p seed sequences, and mutation was generated in the 3′UTR of HOXA1. (E) Luciferase reporter plasmids harbouring the WT or MUT 3′-UTR of HOXA1 were co-transfected with NC agomir or miR-99a-5p agomir into HEK 293 T cells. At 48 h post-transfection, luciferase assay was performed. Data are presented as the mean ± SD. (**$p < 0.01$; ***$p < 0.001$; ns, not significant.)

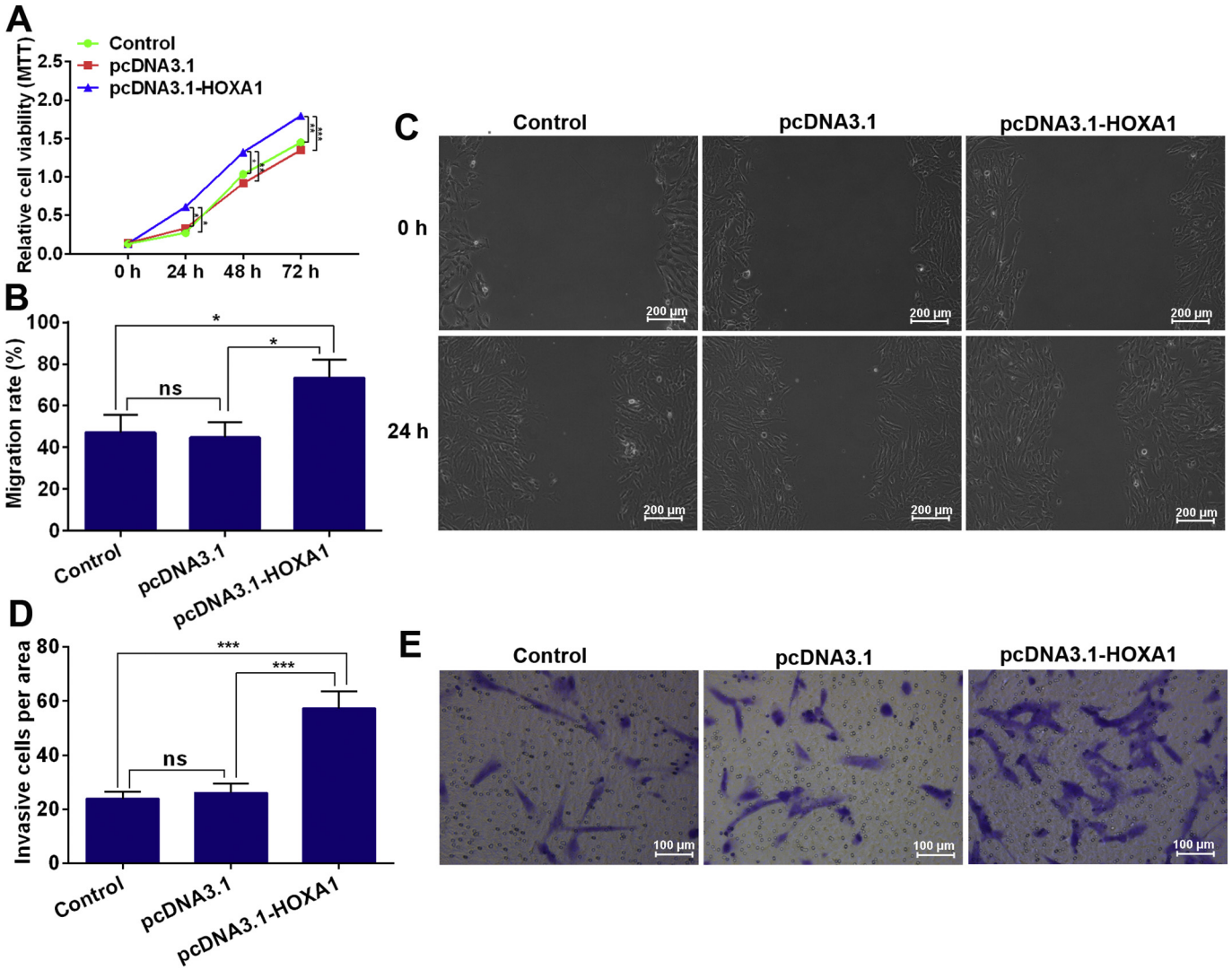


**Fig. 2.** HOXA1 overexpression promotes ASMCs proliferation, migration and invasion. (A) MTT assay showed the proliferation of ASMCs at 0, 24, 48 and 72 h after 24 h of transfection. (B and C) Wound healing assay was used to detect ASMCs migration (100×, bar = 200 μm). (D and E) Transwell assay was conducted to evaluate cell invasion (200×, bar = 100 μm). Data are presented as the mean ± SD. ($^{*}p < 0.05$; $^{**}p < 0.01$; $^{***}p < 0.001$; ns, not significant.)

USA) and successively incubated for 4 h at 37 °C in a humidified 5% $CO_2$ incubator. After that, the supernatant was removed and 150 μl dimethyl sulfoxide (KeyGEN, Nanjing, China) was added to dissolve the formazan crystals for 10 min. The absorbance at 570 nm was measured with a microplate reader (BioTek, Vermont, USA).

### 2.5. Wound healing assay

Wound healing assay was conducted to measure cell migration. The transfected cells were pre-treated in the serum-free medium added with mitomycin (1 μg/ml) for 1 h. Hereafter, the cell monolayer was scraped in a straight line with a pipet tip (200 μl), followed by washing with the serum-free medium to remove cellular debris. Then the cells were cultured in the serum-free medium. Subsequently, photomicrographic images were taken at 0 h and 24 h after scratch using a microscope (Motic, Xiamen, China) to analyse the migration path.

### 2.6. Transwell assay

Transwell assay was performed to detect cell invasion by using a transwell system (Corning, Toledo, America). At 24 h after transfection, the transfected ASMCs ($4 \times 10^3$/well) were placed in the upper chamber with serum-free medium and the bottom chamber was filled with F12K complete medium (Sciencell). Then the transfected cells were allowed to invade for 48 h. After that, cells on the lower side were fixed with 4% paraformaldehyde and stained with 0.5% crystal violet dye solution. The stained cells were counted under an inverted phase contrast microscope (Motic).

### 2.7. Luciferase reporter assay

HOXA1 mutant-type (MUT) was obtained from HOXA1 wild-type (WT) by point mutation technique. HOXA1 WT and MUT sequences were cloned into pmir GLO vector, and the resulting constructs pmirGLO-HOXA1-3′UTR-WT and pmirGLO-HOXA1-3′ UTR-MUT, respectively. Afterwards, HEK 293T cells were transiently co-transfected with pmirGLO-HOXA1-3′ UTR-WT or pmirGLO-HOXA1-3′ UTR-MUT and NC agomir or miR-99a-5p agomir using Lipofectamine 3000 reagents (Invitrogen) according to the manufacturer's instructions. Forty-eight hours after transfection, luciferase activity was determined using the Dual Luciferase Reporter Assay kit (Promega, Madison, WI, USA) according to the manufacturer's instructions.

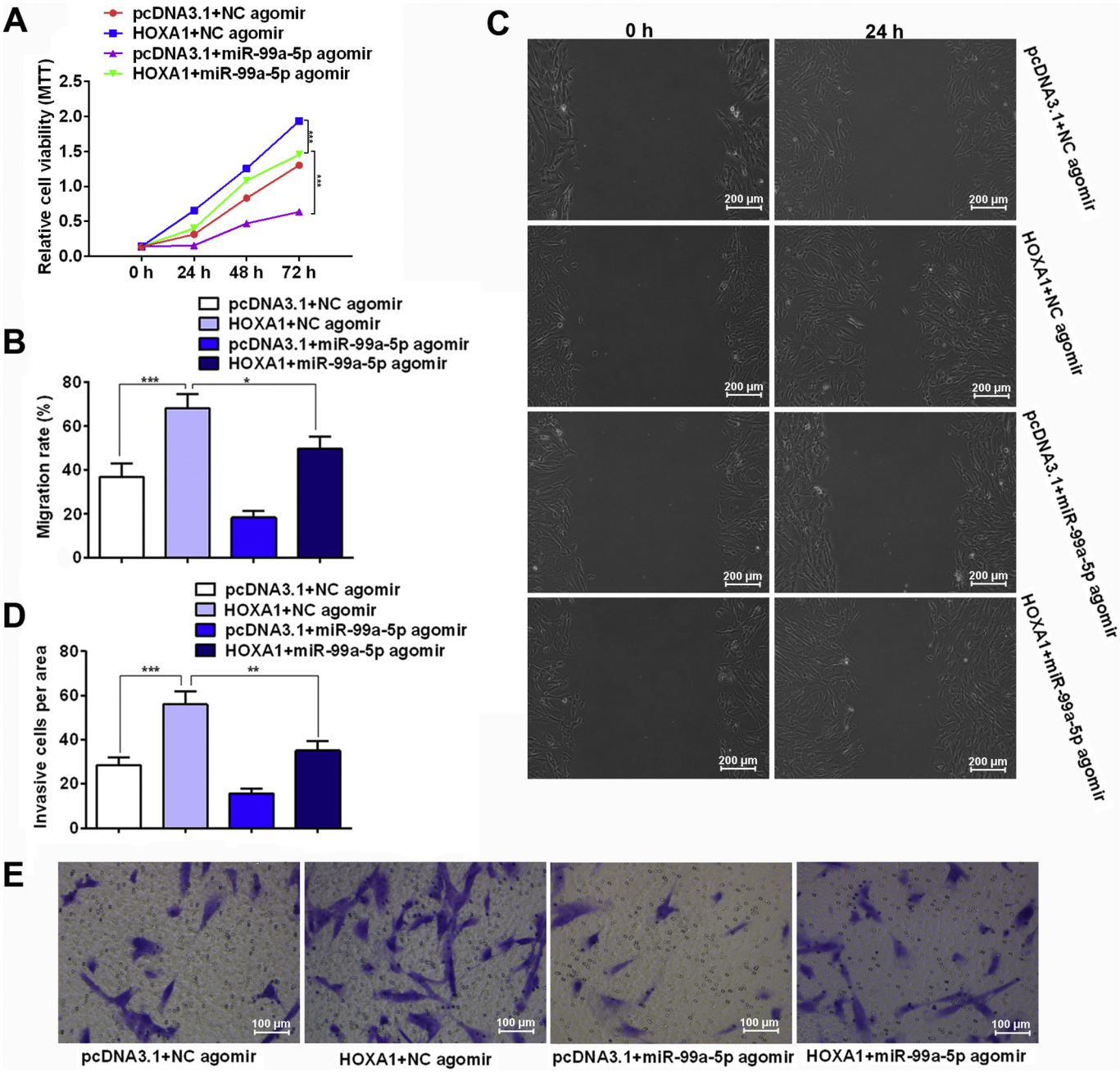


**Fig. 3.** Promotion of the proliferation, migration, and invasion of ASMCs induced by HOXA1 is mediated by miR-99a-5p. ASMCs were transfected with pcDNA3.1 + NC agomir, HOXA1 (pcDNA3.1-HOXA1) + NC agomir, pcDNA3.1 + miR-99a-5p agomir or HOXA1 + miR-99a-5p agomir. (A) The proliferation of ASMCs was tested at 0, 24, 48 and 72 h after 24 h of transfection by MTT assay. (B and C) Wound healing assay was used to detect cell migration (100×, bar = 200 μm). (D and E) Transwell assay was conducted to evaluate cell invasion (200×, bar = 100 μm). Data are presented as the mean ± SD. (*$p < 0.05$; **$p < 0.01$; ***$p < 0.001$.)

### 2.8. Real-time PCR for miRNA and gene mRNA analysis

Total RNAs were extracted from human ASMCs and mouse aortas by using the TRIpure isolation reagent (BioTeke, Beijing, China) according to the manufacturer's instructions. RNA concentration was determined using a NANO 2000 ultraviolet spectrometer (Thermo, Massachusetts, America). Then the size of the mature miR-99a-5p was extended by using a stem-loop reverse transcription primer, GTTGGCTCTGGTGCA GGGTCCGAGGTATTCGCACCAGAGCCAACCACAAG. Different cDNAs were synthesized using super M-MLV reverse transcriptase (BioTeke) and real-time PCR was carried out on an Exicycler 96 Real-Time Quantitative thermal cycler (Bioneer, Daejeon, Korea) using SYBR Green I Master Mix (Solarbio, Beijing, China). $2^{-\Delta\Delta CT}$ threshold method was used to calculate the relative expression of miR-99a-5p and HOXA1 mRNA, which were normalized to the internal control U6 and β-actin respectively. The sequences of primers are shown in Table 1.

### 2.9. Western blot

Total proteins were extracted from ASMCs and mouse aortas using RIPA lysate with 1% PMSF (Beyotime, Beijing, China), then separated by 12% polyacrylamide gels and electrophoretically transferred onto polyvinylidene fluoride membranes. After blocking in 5% non-fat milk dissolved in Tris Buffered Saline with Tween, the membranes were

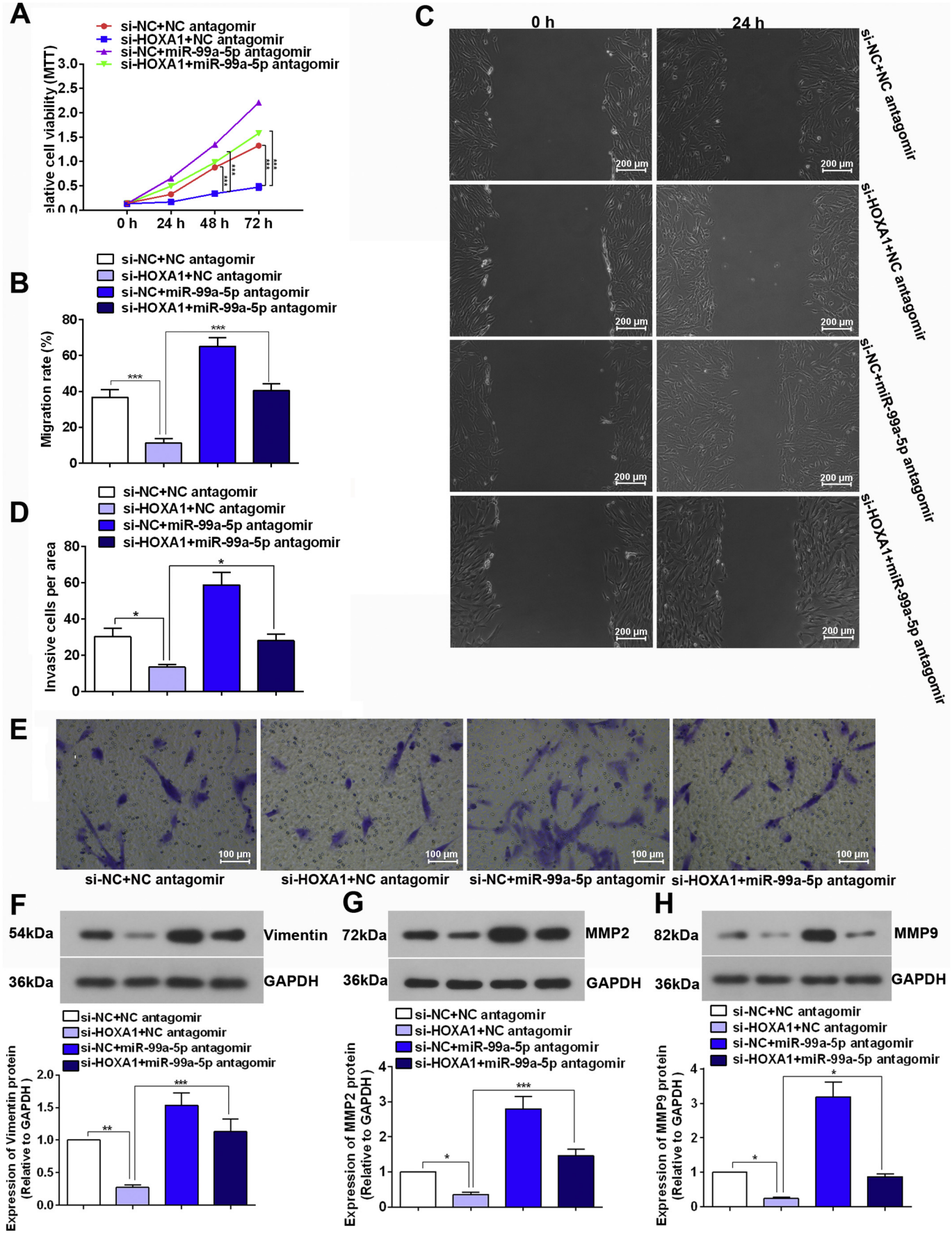


*(caption on next page)*

**Fig. 4.** Inhibition of the proliferation, migration, and invasion of ASMCs by si-HOXA1 is reversed by miR-99a-5p knockdown. ASMCs were transfected with si-NC + NC antagomir, si-HOXA1 + NC antagomir, si-NC + miR-99a-5p agomir or si-HOXA1 + miR-99a-5p antagomir. (A) The proliferation of ASMCs was tested at 0, 24, 48 and 72 h after 24 h of transfection by MTT assay. (B and C) Wound healing assay was used to detect cell migration (100×, bar = 200 μm). (D and E) Transwell assay was conducted to evaluate cell invasion (200×, bar = 100 μm). (F–H) The expressions of migration-related protein Vimentin, MMP2 and MMP9 in ASMCs were determined by western blot assay. Data are presented as the mean ± SD. (*$p < 0.05$; **$p < 0.01$; ***$p < 0.001$.)

incubated with primary antibodies: anti-HOXA1 antibody (1:500, Abcam, Cambridge, UK), anti-β-actin antibody (1:1000, Bioss, Beijing, China), anti-Vimentin antibody (1:2000, Proteintech, Wuhan, China), anti-Matrix Metalloproteinase 2 antibody (MMP2, 1:1000, Proteintech), anti-MMP9 antibody (1:1000, ABclonal, Wuhan, China), anti-GADPH antibody (1:1000, Bioss) at 4 °C overnight. Then membranes were incubated with corresponding HRP-conjugated second antibodies. Finally, all band intensities were visualized using enhanced chemiluminescence reagent (Solarbio) and analysed with the Gel-Pro-Analyzer system.

### 2.10. Animal experiments and grouping

Twelve male apolipoprotein E knockout mice ($ApoE^{-/-}$) and six male C57BL/6J wide-type mice aged 6 weeks were purchased from Beijing Huafukang Bioscience Co., Ltd. (Beijing, China). The animals were bred in a facility with constant humidity and temperature (22 ± 1 °C) under a 12 h light/dark cycle throughout all the experiments. All the experiments were performed according to the Guide for Laboratory Animal Care and Use and approved by the Ethical Committee of Harbin Medical University.

After acclimatization for 1 week, the $ApoE^{-/-}$ mice were randomly divided into two groups: NC agomir group and the miR-99a-5p agomir group. The wide-type mice in the control group were fed with a standard rodent diet for 12 weeks. All $ApoE^{-/-}$ mice were fed a high-fat diet (1.25% cholesterol, 15.8% fat) for 12 weeks. Next, $ApoE^{-/-}$ mice in NC group and miR-99a-5p group received injections of NC agomir and miR-99a-5p agomir (20 mg/kg), respectively, through tail veins twice a week for three weeks. During the 3-week treatment period, the diet of mice in each group was the same as that before treatment. After that, all mice were sacrificed under anesthesia by intraperitoneal injection of sodium pentobarbital (250 mg/kg) and complete aortas were removed for subsequent experiments.

### 2.11. Determination of atherosclerotic lesion

Hematoxylin-eosin (H&E), oil red O, and Masson trichrome staining were performed for histopathological evaluation of the aortic valves. After fixation in 4% paraformaldehyde, the mouse aortic valves were dehydrated in 20% and 30% sucrose solutions successively, and the tissues were submerged into the bottom of the solution indicating complete dehydration. Subsequently, the tissues were embedded in optimal cutting temperature (OCT) compound and were cross-sectioned into 10-μm sections using a freezing microtome (Leica, Solms, Germany). Serial sections were stained with several staining solutions following the manufacturer's instructions. The images were captured under a light microscope (Olympus, Tokyo, Japan) and the Image Pro Plus software was used to analyse the images.

### 2.12. Immunohistochemistry

Immunohistochemistry assay was performed for expression of HOXA1. OCT-embedded tissues were cut on a cryostat (10-μm) then fixed with 4% paraformaldehyde for 15 min, air dried and stored in a refrigerator (−70 °C). Frozen sections were antigen-retrieved, pretreated with 3% hydrogen peroxide and blocked with goat serum for 15 min. Hereafter, the sections were incubated with anti-HOXA1 primary antibody (1:200 dilution, Proteintech, Wuhan, China) at 4 °C overnight and HRP-labeled secondary antibody (1:500 dilution, Thermo Fisher Scientific, Waltham, MA, USA) at 37 °C for 60 min. After a washing stage, the staining was visualized by incubation with DAB solution (Solarbio) and the sections were counterstained with hematoxylin. Finally, the sections were observed under a light microscope (Olympus) at 400× magnification.

### 2.13. Immunofluorescence

Immunofluorescent staining of Cluster of Differentiation 68 (CD68) in atherosclerotic lesion and smooth muscle α-actin (SM α-actin) and smooth muscle 22 alpha (SM-22α) in ASMCs was performed. After pretreatment, the sections were incubated with anti-CD68 (1:50 dilution, Santa Cruz, Dallas, Texas, USA), and the ASMCs were incubated with anti-SM α-actin (1:200 dilution, Proteintech) or SM-22α (1:200 dilution, Proteintech) at 4 °C overnight. Then, the sections or ASMCs were probed with corresponding Cy3-labeled secondary antibody (1:200 dilution, Beyotime) respectively. Nuclei were counterstained with 4′,6-diamidino-2-phenylindole (DAPI) for 10 min. Finally, the staining was observed under a fluorescent microscope at 400× magnification (Olympus).

### 2.14. Statistical analysis

All statistical analyses were carried out using GraphPad Prism version 6 software (GraphPad, La Jolla, CA, USA). Statistical analyses were performed using one-way ANOVA followed by Bonferroni's multiple comparison tests. Differences were considered to be statistically significant when $p < 0.05$.

## 3. Results

### 3.1. MiR-99a-5p inhibits HOXA1 expression and targets the 3′UTR of HOXA1 mRNA

We confirmed the effective overexpression of miR-99a-5p by agomir in ASMCs (Fig. 1A) and further confirmed that the over-expressing miR-99a-5p reduced HOXA1 mRNA and protein levels in ASMCs (Fig. 1B and C). The 3'-UTR of HOXA1 was speculated to contain a complementary region of miR-99a-5p seed sequences (Fig. 1D). Results of the dual-luciferase reporter assay showed that the co-transfection of miR-99a-5p agomir and HOXA1–3'-UTR-WT into HEK 293 T cells could suppress the relative luciferase activity, but the co-transfection of miR-99a-5p agomir and HOXA1–3'-UTR-MUT did not limit the relative luciferase activity, which suggested that miR-99a-5p directly targeted to HOXA1 mRNA. (Fig. 1E).

### 3.2. HOXA1 promotes the proliferation, migration and invasion of human ASMCs

Effect of HOXA1 on cell proliferation of human ASMCs was examined by MTT assay. PcDNA3.1-HOXA1 transfection significantly promoted ASMCs proliferation in a time-dependent manner (Fig. 2A). Additionally, we also evaluated the impact of HOXA1 overexpression on ASMCs migration and invasion, the important events contributing to the progress of atherosclerosis. In wound healing and transwell assays, HOXA1 overexpression induced significant increases in migration (Fig. 2B and C) and invasion (Fig. 2D and E) in the ASMCs compared with the control or vector-transfected ASMCs.

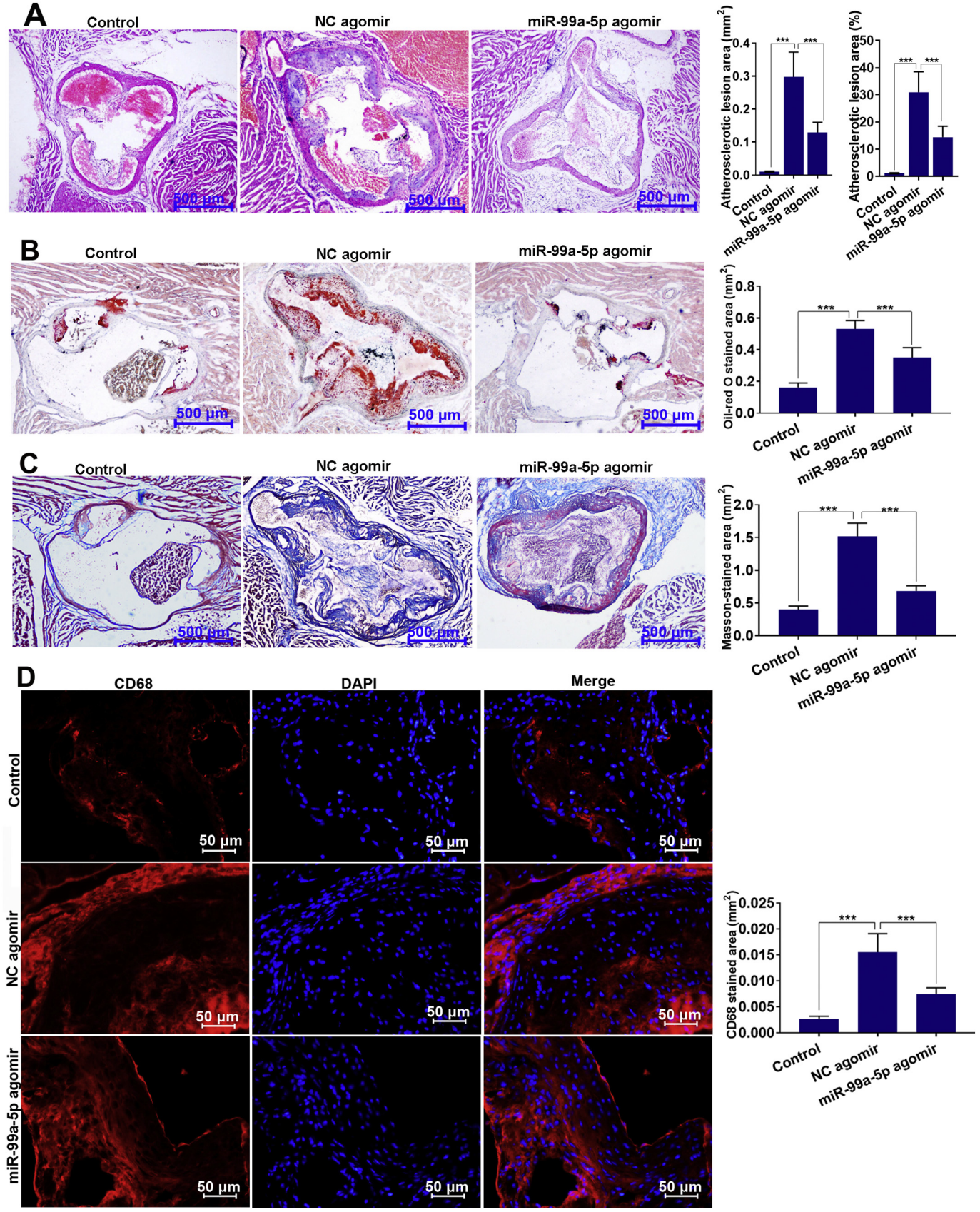


**Fig. 5.** Overexpression of miR-99a-5p alleviates atherosclerotic lesions in the aorta of ApoE$^{-/-}$ mice. Aorta valves from C57BL/6 mice and ApoE$^{-/-}$ mice injected with NC agomir or miR-99a-5p agomir were stained. (A) Hematoxylin and eosin staining, atherosclerotic lesion area and the ratio of atherosclerotic lesion area to the total aorta valves (40×, bar = 500 μm). (B) Oil Red O staining and quantitative analysis (40×, bar = 500 μm). (C) Masson trichrome staining and quantitative analysis (40×, bar = 500 μm). (D) Immunofluorescence staining and quantitative analysis (400×, bar = 50 μm). Data are presented as the mean ± SD. (***$p < 0.001$.) (For interpretation of the references to colour in this figure legend, the reader is referred to the web version of this article.)

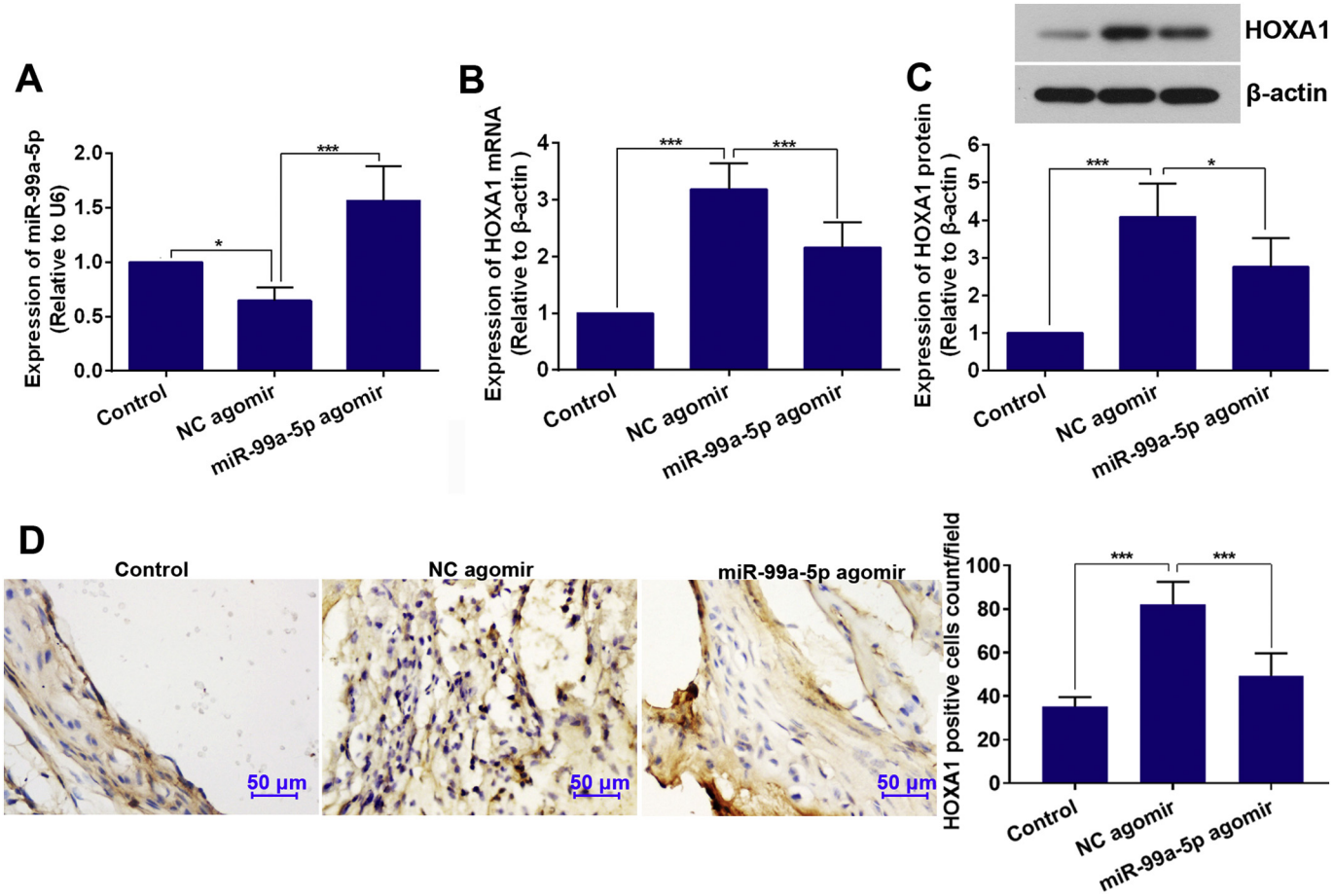


**Fig. 6.** Overexpression of miR-99a-5p downregulates the expression of HOXA1 in the aorta of ApoE$^{-/-}$ mice. (A) Relative miR-99a-5p level of mice in different groups was assessed by real-time PCR. (B and C) Relative mRNA and protein levels of HOXA1 in mice of different groups were assessed by real-time PCR and western blot. (D) Immunohistochemistry and cell count of HOXA1 positive cells. Data are presented as the mean ± SD. (*$p < 0.05$; **$p < 0.01$; ***$p < 0.001$.)

### *3.3. Promotion of ASMCs proliferation, migration and invasion by HOXA1 is counteracted by miR-99a-5p overexpression*

Given the above observations that miR-99a-5p targets HOXA1, we probed whether promotion of proliferation, migration and invasion by HOXA1 was mediated by miR-99a-5p overexpression in ASMCs. HOXA1 transfection markedly promoted ASMCs proliferation, however, enforced miR-99a-5p expression suppressed the HOXA1-stimulated proliferation of ASMC as determined by MTT assay, in particular after 72 h of transfection (Fig. 3A). Indeed, results of wound-healing and transwell assays showed that HOXA1-overexpressing resulted in enforced migratory and invasive abilities, whereas miR-99a-5p overexpression decreased the migratory (Fig. 3B and C) and invasive (Fig. 3D and E) abilities of ASMCs mediated by HOXA1.

### *3.4. Inhibition of the proliferation, migration, and invasion of ASMCs by si-HOXA1 is reversed by miR-99a-5p knockdown*

To further examine the specific relevance of miR-99a-5p to HOXA1, we used si-HOXA1 and miR-99a-5p antagomir to knock down HOXA1 and miR-99a-5p in ASMCs. As presented in Fig. 4A, HOXA1 inhibition by si-HOXA1 markedly suppressed ASMCs proliferation, whereas miR-99a-5p knockdown reversed the effect of si-HOXA1 on the proliferation of ASMCs. Similarly, wound-healing and transwell assays showed that si-HOXA1 suppressed migratory (Fig. 4B and C) and invasive (Fig. 4D and E) abilities of ASMCs, but this inhibitory effect was prevented by miR-99a-5p antagomir transfection. In addition, the expression levels of the key factors MMP-2 and MMP-9, Vimentin in cell migration were measured. As shown in Fig. 4F-H, inhibiting HOXA1 decreased the migration-related proteins, while co-transfection with miR-99a-5p antagomir elevated these protein levels.

### *3.5. Overexpression of miR-99a-5p alleviates atherosclerotic lesions in the aortas of ApoE$^{-/-}$ mice*

To verify the effects of miR-99a-5p on atherosclerosis *in vivo*, an atherosclerotic model was established in ApoE$^{-/-}$ mice. Atherosclerotic mice showed an obvious aortic lesion formation in the aortic valve, but the lesion area was significantly decreased in the corresponding sites of the ApoE$^{-/-}$ mice injected with miR-99a-5p agomir (Fig. 5A). Results of oil red O staining revealed a significant increase in lipid content in atherosclerotic lesion and miR-99a-5p injection reduced lipid deposition (Fig. 5B). Masson trichrome staining results showed increased collagen content in aortic valve of atherosclerotic mice while miR-99a-5p reduced the collagen accumulation (Fig. 5C). We also examined whether miR-99a-5p regulated macrophages accumulation, an important event in the development of atherosclerosis. The expression of the macrophage marker CD68 in aortic valve of ApoE$^{-/-}$ mice or wild type mice was detected by immunofluorescence assay. Similarly, an obvious macrophage accumulation in atherosclerotic mice and a significant reduction in macrophage content within the lesion of miR-99a-5p-treated atherosclerotic mice were observed (Fig. 5D). All these data indicate that enforced miR-99a-5p expression alleviates the atherosclerosis in high-fat diet-fed ApoE$^{-/-}$ mice.

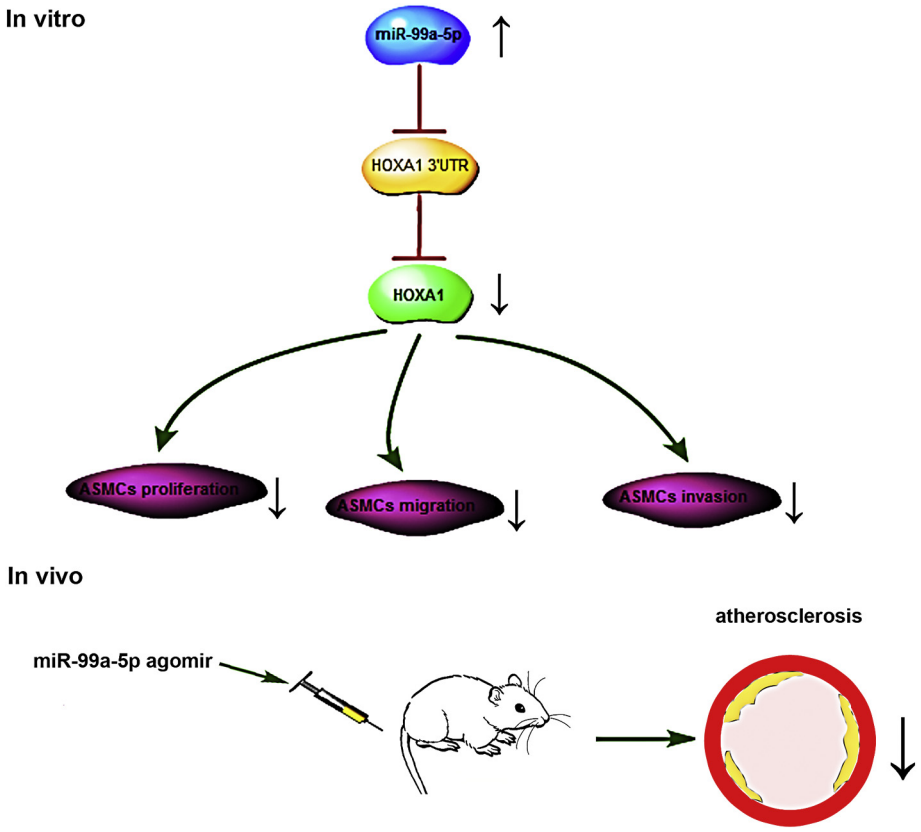


**Fig. 7.** Schematic representation of the mechanism by which miR-99a-5p regulates atherosclerosis by targeting HOXA1. MiR-99a-5p directly targeted HOXA1 and negatively regulated HOXA1 expression. *In vitro*, miR-99a-5p overexpression by miR-99a-5p agomir could inhibit the proliferation, migration, and invasion of ASMCs stimulated by HOXA1, partially through negatively regulating HOXA1. *In vivo*, the specific overexpression of miR-99a-5p by intravenous injection of miR-99a-5p agomir significantly abated atherosclerotic lesions formatted in high-fat diet apolipoprotein E knockout mice.

**Table 2**
Putative target genes of miR-99a-5p.

| Gene name | Gene description | Reference |
|---|---|---|
| MTOR | Mechanistic target of rapamycin (serine/threonine kinase) | [35,36] |
| NOX4 | NADPH oxidase 4 | [37,38] |
| FGFR3 | Fibroblast growth factor receptor 3 | [39] |
| NR6A1 | Nuclear receptor subfamily 6, group A, member 1 | [40] |
| PCSK9 | Proprotein convertase subtilisin/kexin type 9 | [41,42] |
| IGF1R | Insulin-like growth factor 1 receptor | [43] |
| TRIB2 | Tribbles pseudokinase 2 | [44] |
| MTMR3 | Myotubularin related protein 3 | [45] |
| FZD5 | Frizzled class receptor 5 | [46,47] |

### *3.6. Overexpression of miR-99a-5p downregulates the expression of HOXA1 in the aorta of ApoE$^{-/-}$ mice*

We further examined the miR-99a-5p expression in the aortas of mice. The expression of miR-99a-5p was significantly downregulated in ApoE$^{-/-}$ mice injected with NC agomir compared with control animals, but the expression of miR-99a-5p in the ApoE$^{-/-}$ mice was upregulated after injection with miR-99a-5p agomir (Fig. 6A). Subsequently, we validated the effect of miR-99a-5p on expression levels of HOX1 in the aorta. The results showed that the mRNA and protein expression levels of HOXA1 were both notably up-regulated in the high-fat-diet ApoE$^{-/-}$ mice injected with NC agomir compared with the control animals. While miR-99a-5p agomir injection induced a significant reduction of mRNA and protein expression of HOXA1 (Fig. 6B–D), which was consistent with the effect of miR-99a-5p on HOXA1 expression in human ASMCs.

## 4. Discussion

In the present study, we investigated whether miR-99a-5p played an inhibitory effect on atherosclerosis *via* targeting HOXA1. The key findings were as follows: (1) MiR-99a-5p inhibited HOXA1 expression and targeted the 3′UTR of HOXA1 mRNA. (2) Overexpression of HOXA1 resulted in the significant promotion of proliferation, migration and invasion of human ASMCs. (3) MiR-99a-5p inhibited the effects of HOXA1 on ASMCs. (4) MiR-99a-5p downregulated the expression level of HOXA1 and reduced the formation of atherosclerotic lesions in high-fat diet-fed ApoE$^{-/-}$ mice (Fig. 7).

MiRNAs possess multiple features that make them attractive candidates as new prognostic and therapeutic tools for atherosclerosis [23–25]. MiR-99a-5p has been reported to inhibit biological behaviour of VSMCs [10]. It has been reported that miR-99a-5p targets HOXA1 in epithelial cells, nasopharyngeal carcinoma cells and breast cancer cells [18,21,22]. However, HOXA1 expression has not been detected in human ASMCs before. MiR-99a-5p is a regulator of HOXA1 in non-vascular cells. In the present study, we found that miR-99a-5p also inhibited HOXA1 expression and targeted 3′UTR of HOXA1 mRNA. HOXA1, known as an oncogene, plays a role in upregulating tumour cells proliferation, migration *in vitro* and tumour formation *in vivo* [26–29]. Interestingly, a previous study has found that HOX genes are involved in vascular wall-resident multipotent stem cell differentiation into smooth muscle cells, which is critical for vascular disease processes [17]. Similarly, Boström et al. found that Homeobox genes may be involved in human vascular pathology, and they identified that Homeobox B7 was expressed in multipotent clones of bovine aortic medial cells and in human atherosclerotic lesions [30]. In addition, HOXA1 is necessary for the development of pharyngeal arch arteries [31]. In the present study, we showed, for the first time, that overexpression of HOXA1 enhanced proliferation, migration, and invasion in human ASMCs. Furthermore, when HOXA1 was co-transfected with miR-99a-5p into ASMCs, cell proliferation, migration and invasion stimulated by HOXA1 overexpression alone were obviously inhibited. In addition, siRNA mediated HOXA1 knockdown inhibited cell proliferation, migration and invasion in the ASMCs, which could be reversed by

miR-99a-5p antagomir. Our work is consistent with the anti-proliferative and anti-invasive functions of miR-99a-5p described in other studies [8,22]. These data indicate that HOXA1 may be involved in the development of atherosclerotic.

Feinberg et al. have documented miRNA-mediated effects both in atherosclerosis progression and regression [32]. Concernedly, several lines of evidence have indicated that atherosclerotic progression ApoE$^{-/-}$ mice can be inhibited by multiple miRNAs such as miR-let-7g and miR-30c [33,34]. After miR-99a-5p agomir administration, the level of miR-99a-5p in atherosclerotic ApoE$^{-/-}$ mice was increased significantly and the atherosclerotic lesion was significantly alleviated as evidenced by the reduction of atherosclerotic lesion area, lipids and macrophages deposition. Moreover, miR-99a-5p also downregulated HOXA1 protein and mRNA expression levels in the aorta of ApoE$^{-/-}$ mice, which was consistent with the effect of miR-99a-5p on HOXA1 expression in the human ASMCs. These findings suggest that overexpression of miR-99a-5p can attenuate atherosclerosis in HFD-induced ApoE$^{-/-}$ mice, and HOXA1 may be associated with this anti-atherosclerotic effect.

HOXA1 is just one of the numerous target genes of miR-99a-5p. It is possible that other genes regulated by miR-99a-5p also participate in the process of atherosclerosis. Bioinformatics analysis was performed to predict other potential target genes of miR-99a-5p and nine genes were found to be involved in atherosclerosis (Table 2). More specific molecular mechanisms underlying the involvement of miR-99a-5p and its targets in atherosclerosis require further investigation.

## 5. Conclusion

Collectively, miR-99a-5p attenuates atherosclerosis. This effect may be associated with HOXA1 downregulation. MiR-99a-5p may become a potential therapeutic target for atherosclerosis.

Supplementary data to this article can be found online at https://doi.org/10.1016/j.lfs.2019.116664.

## CRediT authorship contribution statement

**Zhiyang Han:**Conceptualization, Data curation, Writing - original draft. **Yinghui Guan:**Visualization, Software. **Bing Liu:**Data curation, Software. **Yu Lin:**Data curation, Visualization. **Yan Yan:**Visualization, Software. **Haijun Wang:**Project administration. **Hengzhen Wang:**Project administration. **Bao Jing:**Conceptualization, Project administration, Writing - review & editing.

## Declaration of Competing Interest

None.

## Acknowledgements

This study was supported by grants from the University Nursing Program for Young Scholar with Creative Talents in Heilongjiang Province, China (No. UNPYSCT-2016193); the Scientific Research Innovation Foundation of Harbin Medical University, China (No. 2017LCZX05); the Scientific Research Innovation Foundation of The First Affiliated Hospital of Harbin Medical University, China (No. 2018B012) and the Natural Science Foundation of Heilongjiang Province, China (No. LH2019H019).

## References

[1] P. Libby, Inflammation in atherosclerosis, Nature 420 (6917) (2002) 868–874, https://doi.org/10.1038/nature01323.
[2] R.R. Packard, P. Libby, Inflammation in atherosclerosis: from vascular biology to biomarker discovery and risk prediction, Clin. Chem. 54 (1) (2008) 24–38, https://doi.org/10.1373/clinchem.2007.097360.
[3] R. Garzon, et al., MicroRNAs in cancer, Annu. Rev. Med. 60 (2009) 167–179, https://doi.org/10.1146/annurev.med.59.053006.104707.
[4] A. Bhardwaj, et al., MicroRNA-based cancer therapeutics: big hope from small RNAs, Mol. Cell. Pharmacol. 2 (5) (2010) 213–219, https://doi.org/10.4255/mcpharmacol.10.27.
[5] M. Liu, et al., MicroRNA let-7g alleviates atherosclerosis via the targeting of LOX-1 in vitro and in vivo, Int. J. Mol. Med. 40 (1) (2017) 57–64, https://doi.org/10.3892/ijmm.2017.2995.
[6] K. Ren, et al., MicroRNA-24 aggravates atherosclerosis by inhibiting selective lipid uptake from HDL cholesterol via the post-transcriptional repression of scavenger receptor class B type I, Atherosclerosis 270 (2018) 57–67, https://doi.org/10.1016/j.atherosclerosis.2018.01.045.
[7] Y. Liu, et al., MiR-99a-5p inhibits bladder cancer cell proliferation by directly targeting mammalian target of rapamycin and predicts patient survival, J. Cell. Biochem. (2018), https://doi.org/10.1002/jcb.27318.
[8] Y. Shi, et al., MiR-99a-5p regulates proliferation, migration and invasion abilities of human oral carcinoma cells by targeting NOX4, Neoplasma 64 (5) (2017) 666–673, https://doi.org/10.4149/neo_2017_503.
[9] H. Qin, W. Liu, MicroRNA-99a-5p suppresses breast cancer progression and cell-cycle pathway through downregulating CDC25A, J. Cell. Physiol. 234 (4) (2019) 3526–3537, https://doi.org/10.1002/jcp.26906.
[10] Z.W. Zhang, et al., MicroRNA-99a inhibits insulin-induced proliferation, migration, dedifferentiation, and rapamycin resistance of vascular smooth muscle cells by inhibiting insulin-like growth factor-1 receptor and mammalian target of rapamycin, Biochem. Biophys. Res. Commun. 486 (2) (2017) 414–422.
[11] S. Lim, S. Park, Role of vascular smooth muscle cell in the inflammation of atherosclerosis, BMB Rep. 47 (1) (2014) 1–7, https://doi.org/10.5483/BMBRep.2014.47.1.285.
[12] D.A. Chistiakov, et al., Vascular smooth muscle cell in atherosclerosis, Acta Physiol. (Oxf.) 214 (1) (2015) 33–50, https://doi.org/10.1111/apha.12466.
[13] T. Saleh Al-Shehabi, et al., Anti-atherosclerotic plants which modulate the phenotype of vascular smooth muscle cells, Phytomedicine 23 (11) (2016) 1068–1081, https://doi.org/10.1016/j.phymed.2015.10.016.
[14] P. Uhrin, et al., Vascular smooth muscle cell proliferation as a therapeutic target. Part 2: natural products inhibiting proliferation, Biotechnol. Adv. 36 (6) (2018) 1608–1621, https://doi.org/10.1016/j.biotechadv.2018.04.002.
[15] D.M. Wellik, Hox patterning of the vertebrate axial skeleton, Dev. Dyn. 236 (9) (2007) 2454–2463, https://doi.org/10.1002/dvdy.21286.
[16] T. Alexander, et al., Hox genes and segmentation of the hindbrain and axial skeleton, Annu. Rev. Cell Dev. Biol. 25 (2009) 431–456, https://doi.org/10.1146/annurev.cellbio.042308.113423.
[17] D. Klein, et al., Hox genes are involved in vascular wall-resident multipotent stem cell differentiation into smooth muscle cells, Sci. Rep. 3 (2013) 2178, , https://doi.org/10.1038/srep02178.
[18] J.G. Wang, et al., MiR-99a suppresses cell invasion and metastasis in nasopharyngeal carcinoma through targeting HOXA1, Onco Targets Ther. 10 (2017) 753–761, https://doi.org/10.2147/ott.s126781.
[19] J. Wardwell-Ozgo, et al., HOXA1 drives melanoma tumor growth and metastasis and elicits an invasion gene expression signature that prognosticates clinical outcome, Oncogene 33 (8) (2014) 1017–1026, https://doi.org/10.1038/onc.2013.30.
[20] Y. Fang, et al., MicroRNA-10a regulation of proinflammatory phenotype in atherosusceptible endothelium in vivo and in vitro, Proc. Natl. Acad. Sci. U. S. A. 107 (30) (2010) 13450–13455, https://doi.org/10.1073/pnas.1002120107.
[21] D. Chen, et al., MicroRNA-99 family members suppress Homeobox A1 expression in epithelial cells, PLoS One 8 (12) (2013) e80625.
[22] X. Wang, et al., MicroRNA-99a inhibits tumor aggressive phenotypes through regulating HOXA1 in breast cancer cells, Oncotarget 6 (32) (2015) 32737–32747, https://doi.org/10.18632/oncotarget.5355.
[23] M. Chen, et al., MicroRNA-145 alleviates high glucose-induced proliferation and migration of vascular smooth muscle cells through targeting ROCK1, Biomed. Pharmacother. 99 (2018) 81–86, https://doi.org/10.1016/j.biopha.2018.01.014.
[24] H.S. Jeong, et al., Synergy of Circulating miR-212 with Markers for Cardiovascular Risks to Enhance Estimation of Atherosclerosis Presence, vol. 12(5), (2017), p. e0177809, https://doi.org/10.1371/journal.pone.0177809.
[25] K. Li, et al., MiR-664a-3p expression in patients with obstructive sleep apnea: a potential marker of atherosclerosis, Medicine (Baltimore) 97 (6) (2018) e9813, , https://doi.org/10.1097/md.0000000000009813.
[26] X. Zhang, et al., Human growth hormone-regulated HOXA1 is a human mammary epithelial oncogene, J. Biol. Chem. 278 (9) (2003) 7580–7590, https://doi.org/10.1074/jbc.M212050200.
[27] H. Wang, et al., HOXA1 enhances the cell proliferation, invasion and metastasis of prostate cancer cells, Oncol. Rep. 34 (3) (2015) 1203–1210, https://doi.org/10.3892/or.2015.4085.
[28] T.Z. Zha, et al., Overexpression of HOXA1 correlates with poor prognosis in patients with hepatocellular carcinoma, Tumour Biol. 33 (6) (2012) 2125–2134, https://doi.org/10.1007/s13277-012-0472-6.
[29] K.M. Mohankumar, et al., HOXA1-stimulated oncogenicity is mediated by selective upregulation of components of the p44/42 MAP kinase pathway in human mammary carcinoma cells, Oncogene 26 (27) (2007) 3998–4008, https://doi.org/10.1038/sj.onc.1210180.
[30] K. Boström, et al., HOXB7 overexpression promotes differentiation of C3H10T1/2 cells to smooth muscle cells, J. Cell. Biochem. 78 (2) (2015) 210–221.
[31] M. Roux, et al., Hoxa1 and Hoxb1 are required for pharyngeal arch artery development, Mech. Dev. 143 (2017) 1–8, https://doi.org/10.1016/j.mod.2016.11.006.
[32] M.W. Feinberg, K.J. Moore, MicroRNA regulation of atherosclerosis, Circ. Res. 118 (4) (2016) 703–720, https://doi.org/10.1161/circresaha.115.306300.
[33] M. Liu, et al., MicroRNA let-7g alleviates atherosclerosis via the targeting of LOX-1

in vitro and in vivo, Int. J. Mol. Med. 40 (1) (2017) 57–64, https://doi.org/10.3892/ijmm.2017.2995.
[34] S. Irani, et al., MicroRNA-30c mimic mitigates hypercholesterolemia and atherosclerosis in mice, J. Biol. Chem. 291 (35) (2016) 18397–18409, https://doi.org/10.1074/jbc.M116.728451.
[35] A. Kurdi, et al., Potential therapeutic effects of mTOR inhibition in atherosclerosis, Br. J. Clin. Pharmacol. 82 (5) (2016) 1267–1279, https://doi.org/10.1111/bcp.12820.
[36] J.B. Jahrling, et al., mTOR drives cerebral blood flow and memory deficits in LDLR$^{-/-}$ mice modeling atherosclerosis and vascular cognitive impairment, J. Cereb. Blood Flow Metab. 38 (1) (2018) 58–74, https://doi.org/10.1177/0271678x17705973.
[37] C. Schurmann, et al., The NADPH oxidase Nox4 has anti-atherosclerotic functions, Eur. Heart J. 36 (48) (2015) 3447–3456, https://doi.org/10.1093/eurheartj/ehv460.
[38] A. Lozhkin, et al., NADPH oxidase 4 regulates vascular inflammation in aging and atherosclerosis, J. Mol. Cell. Cardiol. 102 (2017) 10–21, https://doi.org/10.1016/j.yjmcc.2016.12.004.
[39] S.E. Hughes, Localisation and differential expression of the fibroblast growth factor receptor (FGFR) multigene family in normal and atherosclerotic human arteries, Cardiovasc. Res. 32 (3) (1996) 557–569.
[40] Y. Wang, et al., NR6A1 couples with cAMP response element binding protein and regulates vascular smooth muscle cell migration, Int. J. Biochem. Cell Biol. 69 (2015) 225–232, https://doi.org/10.1016/j.biocel.2015.10.026.
[41] S. Kumar, et al., Accelerated atherosclerosis development in C57Bl6 mice by overexpressing AAV-mediated PCSK9 and partial carotid ligation, Lab. Investig. 97 (8) (2017) 935–945, https://doi.org/10.1038/labinvest.2017.47.
[42] H. Tavori, et al., Human PCSK9 promotes hepatic lipogenesis and atherosclerosis development via apoE- and LDLR-mediated mechanisms, Cardiovasc. Res. 110 (2) (2016) 268–278, https://doi.org/10.1093/cvr/cvw053.
[43] Y. Higashi, et al., Insulin-like growth factor-1 receptor deficiency in macrophages accelerates atherosclerosis and induces an unstable plaque phenotype in apolipoprotein E-deficient mice, Circulation 133 (23) (2016) 2263–2278, https://doi.org/10.1161/circulationaha.116.021805.
[44] C.S. Fox, et al., Genome-wide association of pericardial fat identifies a unique locus for ectopic fat, PLoS Genet. 8 (5) (2012) e1002705, , https://doi.org/10.1371/journal.pgen.1002705.
[45] M. Ghanbari, et al., A genetic variant in the seed region of miR-4513 shows pleiotropic effects on lipid and glucose homeostasis, blood pressure, and coronary artery disease, Hum. Mutat. 35 (12) (2014) 1524–1531, https://doi.org/10.1002/humu.22706.
[46] M.M. Brandt, et al., Endothelial loss of Fzd5 stimulates PKC/Ets1-mediated transcription of Angpt2 and Flt1, Angiogenesis 21 (4) (2018) 805–821, https://doi.org/10.1007/s10456-018-9625-6.
[47] S. Pandey, Chandravati, Wnt signaling cascade in restenosis: a potential therapeutic target of public health relevance in a North American cohort of Nebraska State, Mol. Biol. Rep. 41 (7) (2014) 4549–4554, https://doi.org/10.1007/s11033-014-3325-0.